RESEARCH ARTICLE OPEN ACCESS

Synthesis, Characterisation And Water Permeability Of Mwnt Buckypapers

Hamad N. Altalyan [A], Brian Jones [B], John Bradd [B], Ahmed Ali Alshahrani [C]
a King Fahad Naval Academy, King Abdullaziz Naval Base, Al Jubail, Saudi Arabia
b School of Earth and Environmental Sciences, University of Wollongong, NSW 2522, Australia.
c National Centre for Irradiation Technology, Nuclear Science Research Institute, King Abdullaziz City for Science & Technology.
Corresponding Author: Hamad N. Altalyan

ABSTRACT
Significant work has been conducted to examine the synthesis and characterisation of MWNT buckypapers. Optimisation of the sonication time, electron microscopic investigation, contact angle analysis, electrical properties measurements, mechanical properties testing and surface area analysis were studied and compared to those of corresponding buckypaper membranes containing the same surfactant Triton X-100. Analysis of scanning electron microscopic images of the surfaces of MWNT/Triton X-100 buckypapers revealed that the diameter of their surface pores (65.6 ± 2 nm) was marginally smaller than that of the corresponding materials prepared using MWNTs (80 ± 2 nm). In contrast, the average internal pore diameter of MWNT buckypapers (27.7 ± 2 nm) was found to be slightly higher than that of their MWNT counterparts (24 ± 1 nm), after analysis of binding isotherms derived from nitrogen adsorption/desorption measurements performed on the materials. The average electrical conductivity of MWNT/Triton-X buckypapers reported here (~56 S/cm) was roughly double the average conductivity of MWNT/Triton-X buckypapers mentioned in a previous study (~24 S/cm). Mechanical property measurements in this research displayed significant variation from those obtained from other MWNT buckypapers prepared under the same conditions. The tensile strength, Young's modulus and ductility of the MWNT/Triton X-100 buckypaper prepared in this study were 3.4 ± 0.8 MPa, 0.4 ± 0.2 GPa and 2.4 ± 0.2% respectively.

Keywords:
Buckypaper (BP)
Carbon nanotube (CNT)
Multi-walled carbon nanotube (MWNT)
Nanotechnology

Date Of Submission:18-10-2018 Date Of Acceptance: 04-11-2018

I. INTRODUCTION

The first appearance of CNTs was in 1991 when they were discovered by Iijima [1]. Since CNTs were discovered, they have been widely used in most areas of science and engineering due to their unique physical and chemical properties. CNTs have exhibited a combination of exceptional mechanical, thermal and electronic properties that make them superlative materials for a broad range of applications [2, 3] such as field-emission materials [4], scanning probe microscopy tips, microelectronic devices [3], electrochemical devices [5] and hydrogen storage devices [6]. Nanoparticles such as CNTs have exceptional absorption properties and can be applied to remove chemical and biological pollutants. CNTs met with special attention because of their capabilities for water treatment and their effectiveness against chemical and biological pollutants [7]. In environmental engineering, CNTs are regarded as an excellent media for different adsorbent applications, including: heavy metals [8]; organic compounds inclusive of herbicides [9], chlorinated compounds [10]; disinfection byproducts [11]; endocrine disruptors [12]; biological contaminants including microorganisms [7]; natural organic matter [13]; and cyanobacterial (e.g. microcystin) toxins [14].

Currently, CNTs are produced fundamentally by three techniques: arc discharge, laser ablation and chemical vapour deposition (CVD; [6, 15]). Both arc discharge and laser ablation, theoretically, cannot synthesize CNTs continuously; therefore, the product yield is limited. Additionally, purification steps are essential to separate the tubes from unwanted by-products. These limitations have motivated the

development of gas-phase techniques, such as chemical vapour deposition (CVD), where nanotubes are formed by the decomposition of a carbon-containing gas. The gas-phase technique is amenable to continuous processes since the carbon source is continually replaced by flowing gas. Furthermore, the final purity of the as-produced nanotubes can be fairly high, minimizing following purification steps [3].

Recently, CNTs have attracted extensive attention for using as bio-nanomaterials at both molecular and cellular levels [16]. Nevertheless, the poor dispersion of CNTs in aqueous and organic solvents has prevented extensive application of CNTs in biological fields [17]. Thus, the development of approaches toward the dispersion of CNTs is essential for their applications. To overcome this issue, researchers have made a great effort to improve techniques for modification of CNTs and dispersions of individual CNTs [18]. Mechanical methods involving ultra-sonication are used to fabricate buckypapers. The high energy imparted through the use of an ultrasonic horn allows large bundles of nanotubes to be physically separated and the resulting individual tubes are stabilised through noncovalent inter-actions with dispersant molecules [19]. These dispersions can be filtered using either vacuum or positive pressure which eventually results in formation of the buckypaper [20].

Our aim in this study is to examine the synthesis, characterisation and water permeability of MWNT buckypapers and compare them to those of other corresponding buckypaper membranes containing the same surfactant Triton X-100.

II. MATERIALS AND METHODS

2.1. Reagents

The CNTs used in this investigation were mainly multi-walled thin nanotubes, with 95% C purity, supplied by Nanocyl (Nanocyl-3100). Triton X-100 (T9284; [21]) was supplied by Sigma Aldrich. Dispersion was prepared using Milli-Q water (18 MΩ cm). A hydrophilic 0.22 μm cellulose nitrate [22] membrane filter was provided by Millipore. Only one type of membrane was used as the support material for the preparation of the buckypapers in this project. Small, circular buckypapers were made using polytetrafluoroethylene (PTFE) membranes of ~4.5 cm diameter (with 0.22 μm pores).

2.2. Dispersion preparation

The dispersant used in the preparation of buckypapers was 1% (w/w) Triton X-100. The structure of Triton X-100 can be seen in Fig 1.

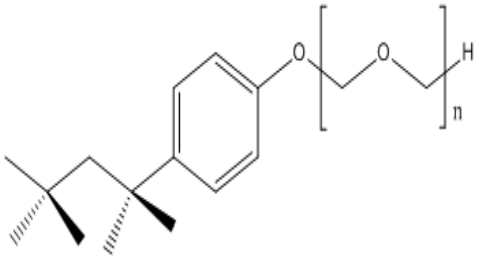

Fig. 1: Structure of the surfactant used as the CNT dispersant (Triton X-100).

The dispersion in this study was prepared with a multi-walled nanotube (MWNT) concentration of 0.1% in accordance with earlier studies. Basically, 15 mg of MWNTs were dispersed in 15 mL of dispersant solution using a Branson 450 (400 W, Ultrasonics Corp.) digital sonicator horn with a probe diameter of 10 mm. A power setting of 30% (120 W) and pulses of 0.5 sec ‘on’ and 0.5 sec ‘off’ were used. The total amount of sonication ‘on’ time (i.e. the amount of time that the horn is energised) was obtained from a series of UV-vis NIR experiments conducted using Triton X-100 dispersions. During sonication, the sample vials containing the MWNTs and dispersant were placed inside an ice water bath to minimise changes in temperature that may happen from the heat generated. The dispersion (1% in Triton X-100) was prepared and added to 50 mL of dispersant solution before being bath sonicated for 3 minutes. The resulting 80 mL dispersion solution containing 30 mg of MWNTs was then diluted to its ultimate volume using Milli-Q water, and was inverted to facilitate complete mixing.

2.3. Buckypaper preparation

`To produce a regular size of buckypapers, circular buckypapers measuring approximately 35 mm in diameter were prepared by using Aldrich glass filtration units. The dispersion was drawn through a membrane filter (0.22 μm pore size; Millipore) under vacuum, produced via a Vacuubrand CVC2 pump, operating between 50 and 100 mbar. The upper part of the filtration unit was covered with plastic film to prevent evaporative losses during the filtration process, which typically took roughly one day. After completion of the filtration process for dispersion, the resulting buckypapers were rinsed with 250 mL of Milli-Q water followed by 10 mL of methanol (99.8%, Merck) while still in the filtration unit. After being rinsed, the damp buckypaper was placed between absorbent paper sheets and allowed to dry for 24 hours. In the final step, the dry buckypaper was then carefully peeled away from the filtration membrane.

2.4. Characterisation techniques

Significant work has been conducted to examine the characterization of MWNT buckypapers. Optimisation of the sonication time, electron microscopic investigation, contact angle analysis, electrical properties measurements, mechanical properties testing, and surface area analysis were examined.

2.4.1. UV-vis-NIR Spectroscopy

An important step that should be considered before the preparation of a buckypaper is to optimise the sonication time used for preparing the CNT dispersion from which the buckypaper will be made. The reason for that is the energy input during the sonication process could lead to shorter CNTs and subsequently will unfavourably impact the mechanical and electrical properties of the resulting buckypaper. Therefore, UV-vis-NIR spectra of the dispersion (Triton-X) was acquired between 1000 and 300 nm using a Cary 500 UV-vis-NIR spectrophotometer. The dispersion (Triton-X) was diluted in quartz cuvettes by adding 2.4 mL of Milli-Q water to a 0.1 mL sample of dispersion and then mixed by inversion to ensure the absorbances were within the optimal range of the instrument.

2.4.2. SEM-EDS and AFM analysis

The surface morphology and cross-section of the prepared buckypapers was examined using a JEOL JSM-7500FA field-emission scanning electron microscope (SEM). Images were analysed using Image Pro Plus software to ascertain quantitative information concerning the size of surface pores. Energy dispersive spectrometer (EDS) analysis was performed in conjunction with imaging using the SEM to provide information on the identity of elements present on the surface of buckypaper samples. The surface topography of membranes was examined by means of atomic force microscopy (AFM).

2.4.3. Contact angle measurement

The contact angles of MWNT buckypapers were measured using the sessile drop technique on a custom device developed by R. Taylor (University of Wollongong) utilising a Dinolite am-211 digital microscope. The contact angles of 2 µL Milli-Q water droplets on the surfaces of the buckypapers were computed utilizing the accompanying Data Physics software (SCA20.1). The mean contact angle was computed using measurements performed on at least five water droplets.

2.4.4. Electrical properties measurements

The electrical conductivity of buckypaper samples was examined according to a standard two-point probe technique [23]. Rectangular strips roughly 3 mm wide and 3–5 cm long were used to test resistance measurements of buckypaper as a function of length. A strip of buckypaper 3 mm wide was connected to pieces of copper tape (3M) on a glass microscope slide using high purity silver paint (SPI). Another glass microscope slide was clamped onto the initial glass slide containing the buckypaper strip using bulldog clips to ensure the sample was protected and a constant force was applied. The I-V characteristics between -0.05 V and 0.05 V were determined using an Agilent waveform generator (33220A) and multi-meter (34410A) connected to the copper tape contacts through a simple circuit. The resistance was computed from the slope of the line in the I-V plot. The strip was shortened and then reconnected to pieces of copper tape on the microscope slide using silver paint before the resistance was measured again. At least 5 lengths were measured for each strip of buckypaper.

2.4.5. Mechanical properties testing

The mechanical properties of buckypapers were measured by using a Shimadzu EZ-S universal testing device and buckypaper samples cut into small rectangular strips measuring 15 mm by 3 mm and attached into a small paper frame. Five different strips were used to determine the tensile strength of buckypapers. The distance between the top and bottom of buckypaper strips was kept constant at 10 mm. The paper frame was cut between the clamps prior to testing, and the attached samples were then stretched by means of a 10 N load cell, at a strain rate of 1 mm min^{-1} until failure. The tensile strength of every single sample was determined as the maximum stress measured. The ductility was determined by taking the percentage elongation (% EL) of the sample at break, and is defined by Equation (1):

$$\text{Ductility} = \frac{l - l_0}{l_0} \times 100 \quad (1)$$

Where l is the length at break and l_0 is the starting length. The Young's modulus of each buckypaper strip was calculated as the slope of the linear part of the stress-strain diagram using the equation (2):

$$E = \frac{\sigma}{\varepsilon} \quad (2)$$

Where E is the Young's modulus (MPa), σ is the stress (MPa) and ε is the strain. The toughness of a sample is described as the area under its stress-strain curve up to the point of fracture [24]. The toughness of each buckypaper was linked to its mass and expressed in units of J/g by dividing the toughness (in J/m^3) by the density of the buckypaper (in g/m^3).

2.4.6. Surface area analysis

Triton-X-100 buckypapers subjected to BET (Brunauer, Emmett, Teller) analysis externally at the King Abdullaziz City for Science & Technology (KACST), Riyadh, Saudi Arabia, to evaluate the surface area of the buckypapers. The samples were annealed underneath argon to burn off the surfactant and cut into small pieces, before being tested using a Micrometric ASAP2010 and a Micrometric ASAP2400.

2.5. Permeability studies

The permeability of buckypapers towards water was performed using a custom-made dead-end filtration cell setup as described in part 3.4.2. Initially, a pressure of 0.15 bar was applied to induce water transport across the buckypaper and then the pressure was increased gradually. Permeate was received in a beaker on top of a computer-controlled balance (Mettler Toledo AB2 with Balancelink 1.0 software).

MWNT buckypapers were examined by means of five or six different flow rates. At each flow rate, the mass of permeate was recorded every second for 5 minutes. The period of each test was kept to a minimum to avoid fouling of the membrane. The flux of water through the buckypaper was then calculated using following Equation:

$$J = \frac{Q}{A\Delta t} \qquad (3)$$

Where J is the permeation flux ($L/m^2.h$), Q is the permeation volume (L) of the testing solution, A is the effective area of the tested substrate (m^2), and Δt is the sampling time (h).

III. RESULTS AND DISCUSSION

3.1. Optimisation of sonication time

Optimisation of the sonication time to disperse MWNTs in Triton X-100 solutions was conducted using UV-vis-NIR spectrophotometry and samples containing 0.1% (w/v) MWNT and 1% (w/v) Triton X-100 which was used as a surfactant. Spectra were obtained after different periods of sonication and are presented in Fig. 4. It is clearly observed that absorbance increases at all wavelengths consistent with increasing sonication time, indicating an increase in the quantity of MWNTs dispersed in the aqueous solution (Fig. 2a).

Fig. 2b displays that extremely dispersed MWNT/Triton X solutions were achieved after very short sonication times. Nonetheless, after 6 min the increase in absorbance became more gradual. After 24 min sonication the absorbance became more stable and there was no notable change to the absorbance at 660 nm. This means that after 24 min sonication, additional dispersion of MWNTs into solution is negligible. Additionally, sonication of samples for longer periods of time could expose the nanotubes to increased amounts of energy, which may cause further degradation of the nanotubes and be accompanied by a decrease in the physical properties of the resulting dispersion. Thus, it can be concluded that 24 min is the optimum sonication time to disperse MWNTs in Triton X-100 solutions.

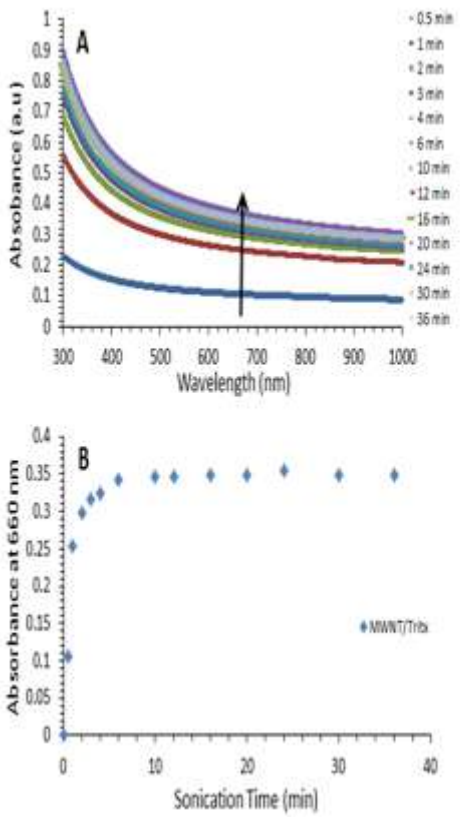

Fig. 2: (a) Absorption spectra of a 0.1% (w/v) MWNT/1% (w/v) Triton-X dispersion taken at different sonication times. (b) Effect of increasing sonication time on the absorbance at 660 nm of the MWNT/Triton X-100 dispersion.

3.2. AFM, SEM and BET analysis

Average roughness was studied by 3D topographic analysis (see Fig. 3 and Fig. 4). The AFM image (Fig. 3) of the carbon nanofibrous films shows that the vertically aligned CNTs have an average diameter of ~294 nm and length of 10 µm. In this image, the brightest area presents the highest point of the membrane surface and the dark regions indicate valleys and this can be seen clearly in Fig. 5 [25]. The amount of MWNTs in the composite membrane is an important factor affecting the morphology, so the image in Fig. 3 indicates that the roughness of the membrane was somewhat smoothed by adding 0.1 wt % MWNT to the composite membrane. This result supports the conclusion reached in a previous study [26]. In this later study the roughness of the MWNT membrane was reduced by adding 0.04 wt % MWNT to the polymer matrix. Following that, the roughness increased significantly after adding 0.2 wt % and once again reduced by adding 0.4 wt %.

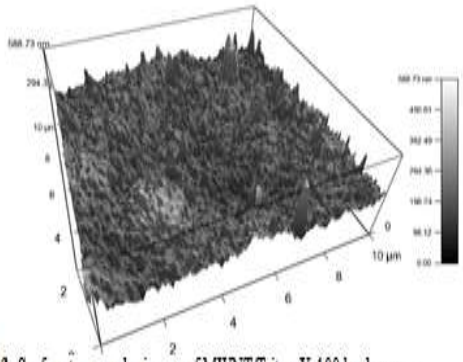

Fig. 3: Surface topography image of MWNT/Triton X-100 buckypaper.

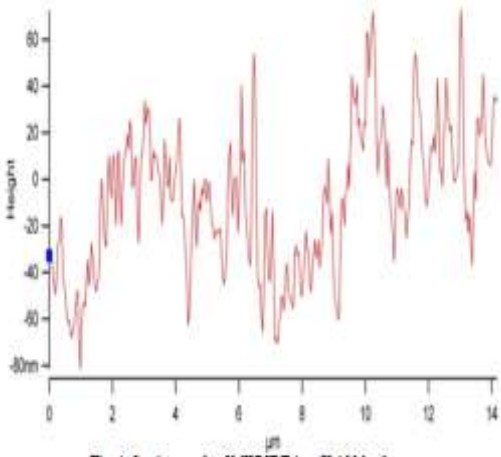

Fig. 4: Section graph of MWNT/Triton X-100 buckypaper.

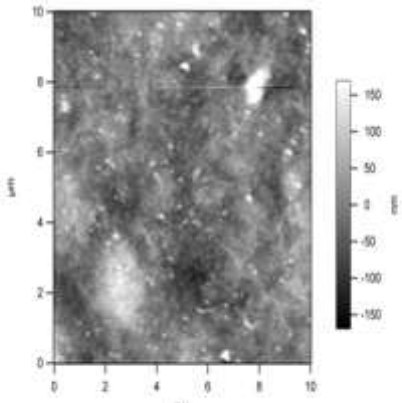

Fig. 5: Plan view image of SIM membrane surfaces reconstructed from AFM roughness statistics for MWNT/Triton X-100 buckypaper.

The surface morphology and cross-section of MWNT buckypapers was studied using a JEOL JSM-7500FA field-emission scanning electron microscopy (SEM). The surface morphology of the MWNT buckypaper seems to be small bundles of tubes with an abundance of small pores (Fig. 6A) and this agrees well with the results of a study conducted by [27]. Also from Fig. 6A, it can be seen that the buckypapers are composed of randomly dispersed MWNTs, which tangle through the van der Waals force and form a uniform porous structure. Furthermore, the cross-sectional image of MWNT buckypaper (Fig. 6B) shows clearly what has been noticed above.

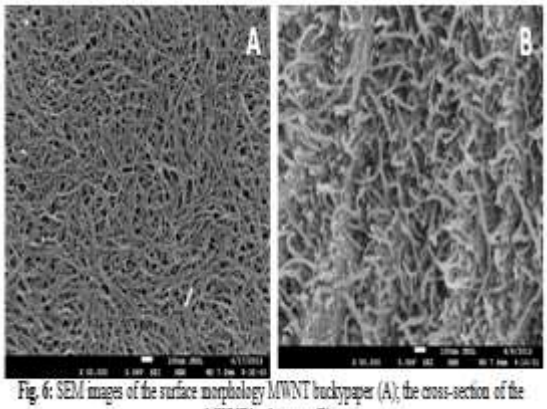

Fig. 6: SEM images of the surface morphology MWNT buckypaper (A); the cross-section of the MWNT buckypaper (B).

More information about the surface area and average internal pore morphology of the MWNT buckypapers was obtained through analysis of the isotherms derived from nitrogen adsorption/ desorption measurements for all MWNT buckypapers and this is demonstrated in Fig. 7. The isotherms obtained for the MWNT/Triton X-100 buckypaper (Fig. 7) exhibit that nitrogen adsorption and desorption occur predominantly at $P/Po > 0.8$. The isotherm for the

MWNT/Triton-X buckypaper in this study is very comparable to those reported previously for other buckypapers prepared using identical conditions [28]. In contrast, the isotherms obtained for the SWNT buckypapers in another study displayed that nitrogen adsorption and desorption occurred at relative pressures (P/Po) below 0.1 can be attributed to the presence of micropores with diameters <2 nm [29].

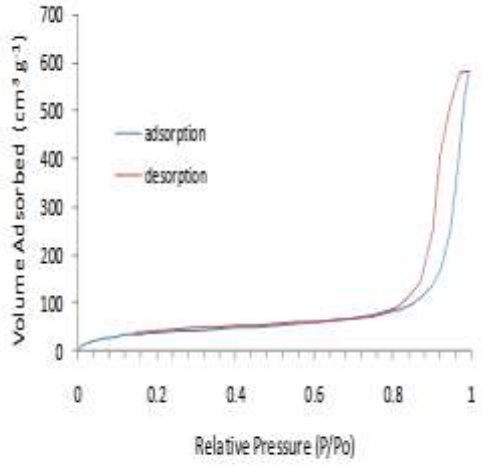

Fig. 7: Nitrogen adsorption (blue)/desorption (red) isotherms for MWNT/Triton X-100.

To investigate the pore structure and surface morphology of MWNT buckypapers, Brunnauer, Emmett and Teller (BET) analysed the results of nitrogen adsorption/desorption measurements. This allowed determination of the specific surface area of the buckypapers and the average pore diameter as well which exists throughout the samples. Table 1 shows surface pore diameter, buckypaper surface area, average internal pore diameter and average nanotube bundle of MWNT buckypapers. If it is assumed that the surface area is related to the outer surface of large CNT bundles, then the bundle diameter (D_{bun}) can be calculated using following equation:

$$A_s = \frac{4}{\rho NT^{D_{bun}}} \qquad (4)$$

where A_s, D_{bun} and ρCNT are the BET surface area, CNT bundle diameter, and nanotube bundle density (estimated as 1500kg/m^3), respectively [30].

The Brunnauer, Emmett and Teller (BET) results presented in Table 1 display large differences in surface area (A_{BET}) and small differences in average internal pore diameter (D_{BET}) to those obtained previously for MWNT buckypaper prepared using Triton X-100, which exhibited a surface area of 300 m^2/g and average pore diameter of 24 ± 1nm [31]. On the other hand, the results obtained for a MWNT/Triton-X buckypaper in this study display a notable difference to those obtained previously for a SWNT/Triton-X buckypaper, which showed a surface area of 794 m^2/g and average internal pore diameter of 4.0 ± 0.4 nm [29]. The interbundle pore volumes determined for the MWNT buckypaper (86 %) is slightly less than what was measured previously for the corresponding membrane composed of MWNT (prepared under the same conditions) and was 91 % [31]. In contrast, the interbundle pore volumes of SWNT buckypaper studied previously was slightly greater than that found in the current study 85 % [29].

Table 1: Morphological properties of MWNT buckypapers

Buckypaper	D_{SEM} (nm)[a]	A_{BET} (m^2/g)[b]	D_{BET} (nm)[c]	D_{bun} (nm)[d]	Interbundle pore volume (%)
MWNT/Trit-100	65.6 ± 60	141 ± 2	27.7 ± 2	19 ± 2	86.4 ± 2
MWNT/Trit-100 (Sweetman's findings)	80 ± 20	300 ± 1	24 ± 1	8.1 ± 0.2	91 ± 5

[a]D_{SEM} surface pore diameter derived by Image Analysis of SEM micrographs. [b]A_{BET}: buckypaper surface area obtained through Brunauer, Emmett and Teller (BET) analysis of isotherms derived from nitrogen adsorption/desorption measurements [32, 33].[c] Average internal pore diameter. [d] Average nanotube bundle diameter. All these parameters compared to findings obtained by [31] for the same type.

To determine the volume of pores with diameters smaller and larger than 3 nm, MWNT buckypapers were subjected to analysis using the Barrett, Joyner and Halendar (BJH) and Horvath-Kawazoe (HK) methods [32, 33]. Analysis by the HK method gave information on the distribution of small pores (<2 nm) within each of the membranes, whereas the BJH method permitted estimation of the larger pores. Combining the two sets of results produced the pore size distribution profiles shown in Fig. 8.

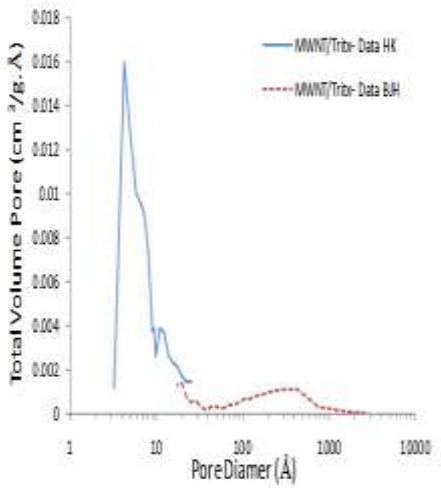

Fig. 8: Pore size distributions for MWNT buckypaper derived by applying the HK method (blue line) and BJH method (brown line) to data obtained from nitrogen adsorption/desorption isotherms.

As seen in Fig. 8, the large peak ranged between 5 and 10 Å consistent with the channels between CNTs within CNT bundles. In contrast, the second peak was nearly 277 Å consistent with the pores formed between CNT bundles. These results agree well with the average pore diameter calculated using BET and shown in Table 1. Numerical combination of curves shown in Fig. 8 was performed to calculate the average internal pore diameter of the membranes, in addition to the percentage contribution of the interbundle pores to the total free volume. The results of this analysis, along with those obtained by use of the BET method are presented in Table 1 [30].

Numerical integration displays that intertube pores contribute ~14% of the total free volume of the buckypaper. Nevertheless, the pores with a diameter larger than 10 Å are linked to the spaces between bundles. The distribution shows peaks at roughly 2 nm and a small tail out to 1000 nm. As they contribute ~86% of the total free volume, the existence of these pores will have a significant impact on the physical properties of the paper as a whole. These results agree well with the results of a similar study which was conducted by [31] who reported that intertube pores contribute ~12% of the total free volume of the MWNT Triton X-100 buckypaper, whereas interbundle pores contribute ~88% of the total free volume of the buckypaper.

3.3. Physical properties of MWNT buckypapers

$$R_T = \frac{1}{\sigma A} l + R_C \qquad (5)$$

Physical properties of MWNT buckypapers include the examination of the electrical properties of MWNT buckypapers (e.g. electrical conductivity and resistant of MWNT) and mechanical properties of MWNT buckypapers (e.g. the tensile strength, Young's modulus and ductility). The electrical properties of MWNT buckypapers are important for separation applications through providing an additional means to exhibit selectivity towards solutes when exposed to an electrochemical potential [34]. The electrical properties are extremely influenced by the filler concentration, the filler morphology (such as particle size and structure) besides filler-filler and filler-matrix interactions which determine the state of dispersion [35]. The 2-point probe technique was employed to measure the conductivity of the MWNT buckypapers prepared in this study. The I-V plots obtained for a MWNT buckypaper prepared using Triton X-100 as the dispersant are presented in Fig. 9. As seen in this figure, the slope of the plots decreased as the length of the strip increased.

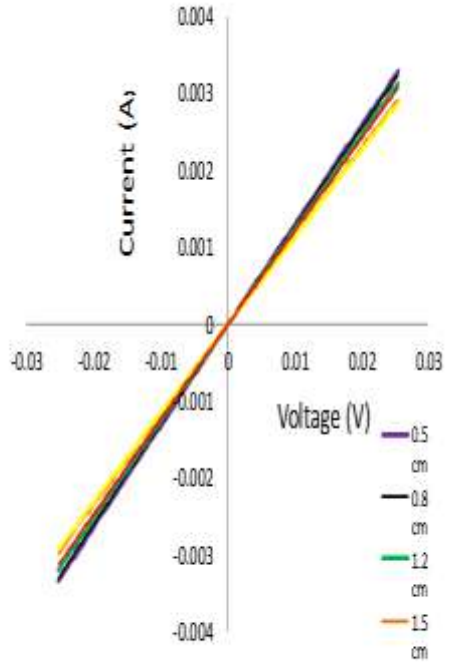

Fig. 9: Current-voltage plots obtained using five different lengths of a strip of gellan gum. The buckypaper was prepared from an 80 mL dispersion using 24 minutes sonication time and filtration through a 0.45 µm nylon membrane.

As the inverse of the slope is equal to the resistance, the resistance was found to increase linearly with strip length. This relationship between the resistance and strip length is presented graphically in Fig. 10. The resistance in the circuit is described through following equation:

Where R_T is the total resistance (Ω), σ is the bulk conductivity (S/cm), A is the strip cross-

sectional area (cm^2), l is the length of the strip (cm) and R_C is the contact resistance (Ω).

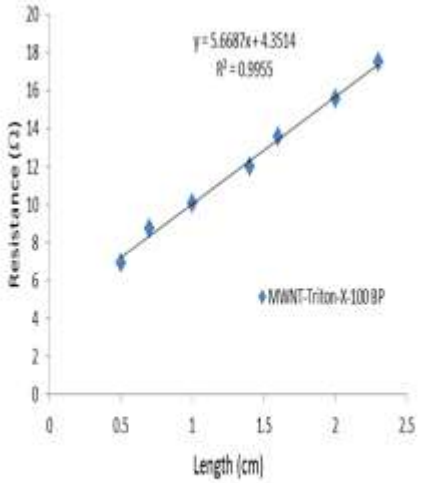

Fig. 10: Effect of length on the resistance of buckypapers prepared from a dispersion containing 0.1% (w/v) MWNT and 1% (w/v) Triton X-100.

Electrical conductivity and resistance of MWNT buckypapers prepared using Triton X-100 are presented in Table 2. As shown in Table 2, electrical conductivity varies significantly (~56 S/cm) from reported by [31] for MWNT buckypapers prepared using the same dispersant and prepared using the same conditions to those used here. In fact the average of MWNT/Triton-X buckypapers reported here was approximately double the average conductivity of MWNT/Triton-X buckypapers which were mentioned in Sweetman et al.'s study. This can be attributed to conditions associated with the manufacturing process of buckypapers, such as the sonication times, the purity and provider of the carbon nanotubes.

3.4. Mechanical properties of MWNT buckypapers

Mechanical strength is an important property of buckypaper membranes for separation applications because the membrane must be able to survive the application using a wide range of pressures and flow rates [36]. An examination of the mechanical properties of the MWNT buckypapers was therefore carried out using the tensile test method and these include the tensile strength, Young's modulus and ductility. These properties were determined for MWNT buckypapers prepared using Triton-x-100 dispersant and are shown in Table 2.

The values displayed in Table 2 vary significantly from those obtained for MWNT buckypapers prepared under the same conditions by Sweetman et al. [31]. For example, the tensile strength, Young's modulus and ductility of a MWNT/Triton X-100 buckypaper prepared in the previous study were 6 ± 3 MPa, 0.6 ± 0.3 GPa and 1.3 ± 0.2 %, respectively.

Table 2: Physical properties of buckypapers. Values shown are the average of at least 3 samples, with the errors reported determined from the standard deviation obtained from all measurements.

Membrane	Tensile strength (MPa)	Young's modulus (GPa)	Ductility (%)	Thickness (μm)	Electrical conductivity (S/cm)	Resistant (Ω)	Contact angle (°)
MWNT/Triton X-100	3.4 ± 0.8	0.4 ± 0.2	2.4 ± 0.2	48 ± 2	56 ± 3	5.4 ± 0.3	50.7 ± 4

The elongation and toughness of a MWNT/Triton X-100 buckypaper prepared in this study was 2.4 ± 0.2% and 0.05 ± 0.01 MJ/m^3, respectively. On the other hand, the elongation and toughness of a MWNT/Triton X-100 buckypaper prepared in another study were 8.89 ± 0.94% and 0.69 ± 0.12 MJ/m^3, respectively [37].

3.5. Hydrophobicity of MWNT buckypapers

To measure the hydrophobicity of material, commonly the contact angle of a water droplet on its surface is used. A data physics SCA goniometer fitted with a digital camera, combined with the data physics software package SCA20.a was used to determine the contact angle of 2 μL water (Milli-Q, Millipore) droplets on the surface of the buckypapers. In the case of measurements performed using water droplets, small contact angles (< 90°) indicate that the surface of the material is hydrophilic, whereas large angles (> 90°) show that the material is hydrophobic in nature. The contact angles for all MWNTs buckypapers examined in this study were measured using 2 μL water droplets delivered via a syringe, as shown in Fig. 11.

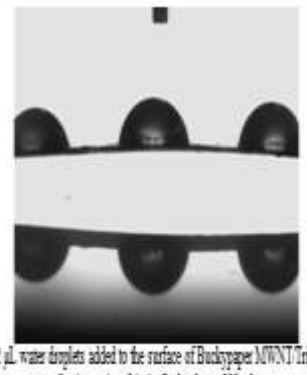

Fig. 11: Images of 2 μL water droplets added to the surface of Buckypaper MWNT/Triton X-100 0.6% w/v, Sonicator time 24min final volume 500 ml.

The mean contact angle of water on MWNT buckypapers calculated based on measurements performed using 5 water droplets is 51°, indicating that their surfaces are in general hydrophilic in nature (Table 2). This agrees well with the results of a similar study by Alcock [38] who reported a water contact angle of 55° for MWNT buckypapers produced from dispersions containing the surfactant Triton-X [31].

3.6. Water permeability experiments of MWNT buckypapers

One of the main considerations that should be taken into account when evaluating a potential filtration membrane is its permeability, particularly towards water. Consequently the first objective of this stage of this study was to quantify the permeability of MWNT buckypapers made with Triton-x-100. The second objective was to compare the measured permeability in this study with previous studies [38, 39]. To achieving this, small buckypapers were examined. Each buckypaper studied became permeable to water after around 14 kPa of positive pressure was applied. The flux of water across all buckypapers usually looks like that shown in Fig. 12 with a linear correlation between the mass of permeate and time being observed.

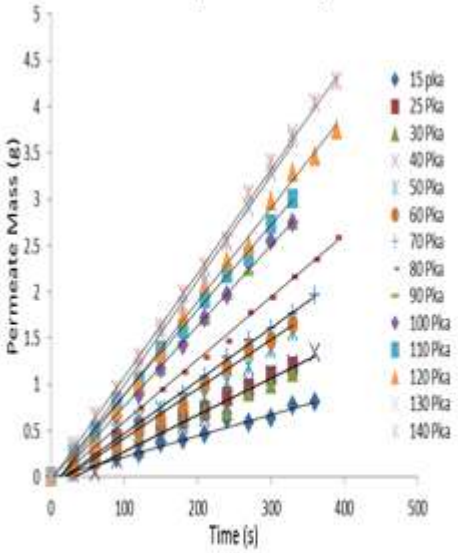

Fig. 12: Effect of pressure on the mass of water permeating across a MWNT/Triton X-100 buckypaper. The slopes of the individual plots give the permeation flux. Data for only selected pressures are shown.

The permeate flux was noticed to increase for all buckypapers as a function of applied pressure until membrane rupture occurred. The slopes of the lines shown in Fig. 12 were then plotted as a function of the applied pressure to provide the graph shown in Fig. 13. From the resulting linear plot the membrane flux was calculated from the slope, after correcting for the actual filtration area. This yielded a flux of 23 L m^{-2} h^{-1} bar^{-1} for MWNT/Triton-x-100 buckypaper. The membrane flux of the MWNT buckypaper prepared in this study is presented in Table 3, along with the membrane fluxes obtained by [38] and [39] for the same type of buckypaper for comparison.

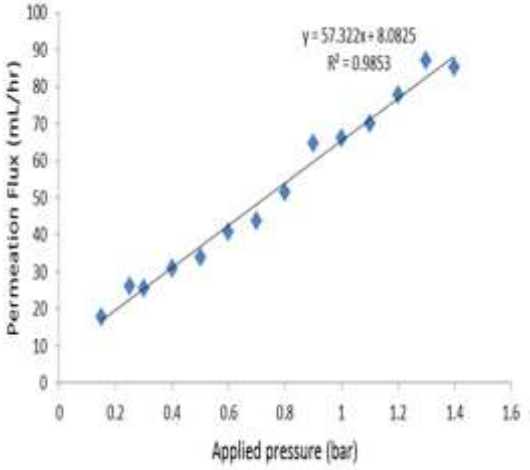

Fig. 13: Effect of applied pressure on the permeation flux of a MWNT/Triton-X buckypaper.

Table 3: Average membrane fluxes determined for MWNT/Triton X-100 compared to the average membrane fluxes obtained by Alcock [38] and Wise [39] for the same type.

Buckypaper	Average flux ($L m^{-2} h^{-1} bar^{-1}$)	Alcock's average flux ($L m^{-2} h^{-1} bar^{-1}$)	Anthony's average flux ($L m^{-2} h^{-1} bar^{-1}$)
MWNT-Triton-x-100	22.9 ± 0.14	22.4 ± 6.3	22 ± 6

IV. CONCLUSION

Buckypaper membranes were successfully fabricated from aqueous dispersions containing MWCNTs and Triton-x-100 and significant characterization work has been conducted to examine these buckypapers as well. Analysis of scanning electron microscopic images of the surfaces of MWNT/Triton X-100 buckypapers revealed that the diameter of their surface pores (65.6 ± 2 nm) was slightly smaller than that of the corresponding materials prepared using MWNTs (80 ± 2 nm). In contrast, the average internal pore diameter of MWNT buckypapers (27.7 ± 2 nm) was found to be marginally higher than that of their MWNT counterparts (24 ± 1 nm), after analysis of binding isotherms derived from nitrogen adsorption/desorption measurements performed on the materials. The buckypapers were permeable towards water and this is consistent with the results which were reported in previous studies. The

mechanical and electrical properties of MWNT buckypapers varied significantly from those obtained for MWNT buckypapers prepared under the same conditions which were mentioned in previous studies. It may be attributed to the sonication times. The previous study reported that changing the sonication times could affect the mechanical properties of BP membranes [40]. A series of BPs were fabricated from dispersions made using different sonication times from 15–60 min, and were then subjected to mechanical properties tests. Additionally, the previous study is exhibited that the tensile strength of buckypaper membranes fabricated from CNTs was significantly enhanced only when high molecular mass surfactants (e.g. proteins or polysaccharides), which intercalated between CNTs to increase the number of tube-to-tube junctions and hence increasing mechanical properties of these buckypaper membranes [41]. Furthermore, the purity and provider of the carbon nanotubes could play a significant role in existence like this variation.

ACKNOWLEDGEMENTS

The authors acknowledge financial support from the Ministry Defence in Saudi Arabia and the Royal Saudi Naval Forces. The authors extend special thanks to all staff and students at the Soft Materials Group, School of Chemistry, University of Wollongong, in particular Assoc. Prof. Marc in het Panhuis, Assoc. Prof. Stephen Ralph, Ahmed Alshahrani, Holly and Leighton. The authors would also like to thank King Abdullaziz City for Science and Technology for assistance obtaining the surface area analysis (BET). The authors are greatly indebted to Mr Tony Romeo in the Electron Microscopy Centre, University of Wollongong for his assistance and support with scanning electron microscope (SEM) images.

REFERENCES

[1]. Iijima, S., Helical microtubules of graphitic carbon. Nature, 1991. **354**(6348): p. 56-58.
[2]. Coleman, J.N., et al., Small but strong: A review of the mechanical properties of carbon nanotube–polymer composites. Carbon, 2006. **44**(9): p. 1624-1652.
[3]. Thostenson, E.T., Z. Ren, and T.-W. Chou, Advances in the science and technology of carbon nanotubes and their composites: a review. Composites Science and Technology, 2001. **61**(13): p. 1899-1912.
[4]. Liu, J., et al., Field emission from combined structures of carbon nanotubes and carbon nanofibers. Physica B: Condensed Matter, 2010. **405**(11): p. 2551-2555.
[5]. Baughman, R.H., A.A. Zakhidov, and W.A. De Heer, Carbon nanotubes--the route toward applications. Science, 2002. **297**(5582): p. 787-792.
[6]. Oriňáková, R. and A. Oriňák, Recent applications of carbon nanotubes in hydrogen production and storage. Fuel, 2011. **90**(11): p. 3123-3140.
[7]. Upadhyayula, V.K.K., et al., Application of carbon nanotube technology for removal of contaminants in drinking water: a review. Science of The Total Environment, 2009. **408**(1): p. 1-13.
[8]. Tofighy, M.A. and T. Mohammadi, Adsorption of divalent heavy metal ions from water using carbon nanotube sheets. Journal of Hazardous Materials, 2011. **185**(1): p. 140-147.
[9]. Yuan, W., et al., Deposition of silver nanoparticles on multiwalled carbon nanotubes grafted with hyperbranched poly (amidoamine) and their antimicrobial effects. The Journal of Physical Chemistry, 2008. **112**(48): p. 18754-18759.
[10]. Yang, K. and B. Xing, Desorption of polycyclic aromatic hydrocarbons from carbon nanomaterials in water. Environmental Pollution, 2007. **145**(2): p. 529-537.
[11]. Lu, C., Y.-L. Chung, and K.-F. Chang, Adsorption of trihalomethanes from water with carbon nanotubes. Water Research, 2005. **39**(6): p. 1183-1189.
[12]. Pan, B., K. Sun, and B. Xing, Adsorption kinetics of 17-ethinyl estradiol and bisphenol A on carbon nanomaterials. II. Concentration-dependence. Journal of Soils and Sediments, 2010. **10**(5): p. 845-854.
[13]. Lu, C. and F. Su, Adsorption of natural organic matter by carbon nanotubes. Separation and Purification Technology, 2007. **58**(1): p. 113-121.
[14]. Yan, H., et al., Adsorption of microcystins by carbon nanotubes. Chemosphere, 2006. **62**(1): p. 142-148.
[15]. Popov, V.N., Carbon nanotubes: properties and application. Materials Science and Engineering: R: Reports, 2004. **43**(3): p. 61-102.
[16]. Lamprecht, C., Torin Huzil, J., V. Ivanova, Marina., Foldvari, Marianna, Non-Covalent Functionalization of Carbon Nanotubes with Surfactants for Pharmaceutical Applications - A Critical Mini-Review. Drug Delivery Letters, 2011. **1**: p. 45-57.

[17]. M.S. Digge, R.S.M., S.G. Gattani,, Applications of carbon nanotubes in drug delivery: a review. International journal of pharmtech research, 2012. **4**(2): p. 839-847.
[18]. Ling, X., et al., Functionalization and dispersion of multiwalled carbon nanotubes modified with poly-l-lysine. Colloids and Surfaces A: Physicochemical and Engineering Aspects, 2014. **443**: p. 19-26.
[19]. De-Quan Yang , J.-F.R., and Edward Sacher Functionalization of multiwalled carbon nanotubes by mild aqueous sonication. The Journal of Physical Chemistry, 2005. **109** (16): p. 7788–7794.
[20]. Shunji Bandow, A.M.R., K. A. Williams, A. Thess, R. E. Smalley and P. C. Eklund,, Purification of single-wall carbon nanotubes by microfiltration. The Journal of Physical Chemistry., 1997. **101**(44): p. 8839–8842.
[21]. Dolar, D., et al., Removal of emerging contaminants from municipal wastewater with an integrated membrane system, MBR–RO. Journal of Hazardous Materials, 2012. **239–240**(0): p. 64-69.
[22]. Loncnar, M., et al., Fate of saline ions in a planted landfill site with leachate recirculation. Waste Management, 2010. **30**(1): p. 110-118.
[23]. Blighe, F.M., et al., Observation of percolation-like scaling-far from the percolation threshold-in high volume fraction, high conductivity polymer-nanotube composite films. Advanced Materials, 2007. **19**: p. 4443-4447.
[24]. Callister, W.D. and D.G. Rethwisch, Materials science and engineering: an introduction. 8th ed ed. 2010.
[25]. Ahmed, S.F., et al., Effect of temperature on the electron field emission from aligned carbon nanofibers and multiwalled carbon nanotubes. Applied Surface Science, 2007. **254**(2): p. 610-615.
[26]. Vatanpour, V., et al., Fabrication and characterization of novel antifouling nanofiltration membrane prepared from oxidized multiwalled carbon nanotube/polyethersulfone nanocomposite. Journal of Membrane Science, 2011. **375**(1–2): p. 284-294.
[27]. Cottinet, P.J., et al., Electromechanical actuation of buckypaper actuator: material properties and performance relationships. Physics Letters A, 2012. **376**(12–13): p. 1132-1136.
[28]. Rashid, M.H.-O., et al., Synthesis, properties, water and solute permeability of MWNT buckypapers. Journal of Membrane Science, 2014. **456**(0): p. 175-184.
[29]. Sweetman, L., Synthesis, Characterisation and Applications of Carbon Nantube Membrane Containing Macrocycles and Antibiotics, in School of Chemistry 2012, University of Wollongong, Wollongong: Wollongong. p. 188.
[30]. Frizzell, C., et al., Reinforcement of macroscopic carbon nanotube structures by polymer intercalation: the role of polymer molecular weight and chain conformation. Physical Review B, 2005. **72**: p. 245420,1-8.
[31]. Sweetman, L.J., et al., Bacterial filtration using carbon nanotube/antibiotic buckypaper membranes Journal of Nanomaterials, 2013. **2013**: p. 781212, 1-11.
[32]. Barrett, E.P., L.G. Joyner, and P.P. Halenda, The determination of pore volume and area distributions in porous substances. I. Computations from nitrogen isotherms. Journal of the American Chemical Society, 1951. **73**: p. 373–380.
[33]. Horvath, G. and K. Kawazoe, Method for the calculation of effective pore size distribution in molecular sieve carbon. Journal of Chemical Engineering of Japan, 1983. **16**: p. 470 - 475.
[34]. Vecitis, C.D., et al., Electrochemical multiwalled carbon nanotube filter for viral and bacterial removal and inactivation. Environmental Science and Technology, 2011. **45**: p. 3672 - 3679.
[35]. Bokobza, L., Multiwall carbon nanotube elastomeric composites: a review. Polymer, 2007. **48**(17): p. 4907-4920.
[36]. He, D. and M. Ulbricht, Surface-selective photo-grafting on porous polymer membranes via a synergist immobilization method. Journal of Materials Chemistry, 2006. **16**: p. 1860 - 1868.
[37]. Han, J.-H., et al., CNT buckypaper/thermoplastic polyurethane composites with enhanced stiffness, strength and toughness. Composites Science and Technology, 2014. **103**(0): p. 63-71.
[38]. Alcock, L., Characterization and Transport Study Involving Multi-Walled Carbon Nanotube Membranes, in School of Chemistry. 2010, University of Wollongong: Wollongong.
[39]. Wise, A., Carbon Nanotube Membranes for Filtration, in School of Chemistry. 2011, Univercity of Wollongong: Wollongong.
[40]. Sweetman, L.J., Synthesis, characterisation and applications of carbon nanotube membranes containing macrocycles and

antibiotics. 2012, Dissertation/Thesis,School of Chemistry, Wollongong University.

[41]. Boge Jenny, et al., The effect of preparation conditions and biopolymer dispersants on the properties of SWNT buckypapers. J. Mater. Chem, 2009. **19,** : p. 9131–9140

Hamad N. Altalyan "Synthesis, Characterisation And Water Permeability Of Mwnt Buckypapers '"International Journal of Engineering Research and Applications (IJERA) , vol. 8, no.10, 2018, pp 58-69